Ionic Diffusion and the Topological Origin of Fragility in Silicate Glasses

ARTICLE *in* THE JOURNAL OF CHEMICAL PHYSICS · DECEMBER 2009

Impact Factor: 2.95 · DOI: 10.1063/1.3276285 · Source: PubMed

3 AUTHORS, INCLUDING:

Morten M Smedskjaer
Aalborg University
79 PUBLICATIONS **790** CITATIONS
SEE PROFILE

Yuanzheng Yue
Aalborg University
209 PUBLICATIONS **2,715** CITATIONS
SEE PROFILE

Ionic diffusion and the topological origin of fragility in silicate glasses

Morten M. Smedskjaer,[1] John C. Mauro,[2] and Yuanzheng Yue[1,a)]
[1]*Section of Chemistry, Aalborg University, DK-9000 Aalborg, Denmark*
[2]*Science and Technology Division, Corning Incorporated, Corning, New York 14831, USA*

(Received 6 October 2009; accepted 1 December 2009; published online 30 December 2009)

Mass transport in liquids and glass is intimately connected to the structure and topology of the disordered network. To investigate this problem, we measure the ionic diffusivity and fragility of a series of iron-bearing alkali-alkaline earth silicate glasses, substituting different types of alkali and alkaline earth cations while keeping the same ratio of network modifiers. Diffusion is studied around the glass transition temperature (T_g) under a reducing atmosphere, leading to a reduction of Fe^{3+} to Fe^{2+}, and inward diffusion of the modifier cations. In the $SiO_2-CaO-Fe_2O_3-A_2O$ (A=Na, K, Rb, or Cs) glass series, we find that the Ca^{2+} ions diffuse faster than alkali ions and that the activation energy of the Ca^{2+} diffusion decreases with alkali size, a trend that is coincident with a decrease in liquid fragility. We have established a simple model for accurately describing the correlation between the fragility index (m) and T_g based on a topological consideration of the glass network. The model builds on a temperature-dependent constraint approach where the Vogel temperature serves as a rigidity percolation threshold. This follows from our derivation of the Vogel–Fulcher–Tammann equation of viscosity from the more accurate Mauro–Yue–Ellison–Gupta–Allan equation. The established model provides an excellent prediction of the relationship between fragility and T_g, except for the MgO-containing glass where Mg^{2+} is known to play a unique topological role in the network. This trend is in coincidence with the considerably faster inward diffusion of Mg^{2+} in comparison to other alkaline earth cations. © *2009 American Institute of Physics*.
[doi:10.1063/1.3276285]

I. INTRODUCTION

A physical understanding of diffusion processes in supercooled liquids and glasses is of great scientific and technological importance. The mass transport properties of a glass are a direct result of the interplay among structure, topology, kinetics, and thermodynamics. It is particularly important to study the diffusion processes in the glass transition range, which corresponds to the onset of ergodic breakdown in a glass-forming liquid. A fundamental understanding of glass behavior requires knowledge of the nonequilibrium physics involved in the glass formation and relaxation processes. Since glass is in an unstable nonequilibrium condition, it will relax spontaneously toward the metastable supercooled liquid state. Within the glass transition region, the relaxation process can be observed directly on a laboratory time scale. The relaxation process is the sum of multiple processes occurring over a range of different time scales. It is therefore important to obtain quantitative data for both slow and fast diffusion mechanisms in glasses. Furthermore, it is important to study diffusion since it affects glass properties such as electrical conductivity, viscosity, thermal expansion, and chemical durability. Through diffusion processes, it is also possible to create new glass surfaces with enhanced chemical durability and hardness.[1,2]

Of course, diffusion behavior can only be measured by employing some method to induce the diffusion process. We have recently established a method to obtain diffusion data of the fast ions (i.e., the network-modifying cations) in the glass transition range.[2,3] The method is also of technological interest since a silica-rich surface layer is created as a consequence of the diffusion. The method is based on a reduction-inward diffusion route. Reduction of a polyvalent element from a higher valence state to a lower valence state (e.g., Fe^{3+} to Fe^{2+}) in silicate glasses takes places under exposure to certain types of gases at the glass transition temperature (T_g). Such reduction drives an inward diffusion (from surface toward the interior) of modifying ions, which in turn leads to the formation of a silica-rich surface layer. The reduction proceeds via two simultaneous processes: gaseous (e.g., H_2) permeation and outward flux of electron holes. To maintain charge neutrality, the latter process requires an inward diffusion of mobile cations. The silica-rich surface layer enhances chemical durability and hardness.[2,3] The mechanism of the inward diffusion has been described in detail elsewhere.[2,3] It has also been reported that the inward diffusion occurs above the liquidus temperature of silicates.[4]

With this method, we have found that the alkaline earth ions exhibit faster diffusion compared to the alkali ions. Normally, alkali ions are found to be faster in silicate glasses due to their lower charge in comparison to alkaline earth ions.[5,6] In this study, we investigate the universal behavior of the inward cationic diffusion process by addressing the following questions:

- What is the impact of the alkali ion on the diffusivity of alkaline earth ions?

a)Electronic mail: yy@bio.aau.dk.

TABLE I. Chemical composition, radius r_A of the alkali ions, density, molar volume, glass transition temperature T_g, and fragility index m of the prepared glasses.[a]

Glass	A	Chemical composition (mol %) SiO_2	CaO	Fe_2O_3 [b]	A_2O	r_A (Å)	Density (g/cm^3)	Molar volume (cm^3/mol)	T_g (K)	m (-)
Si–Ca–Fe–Na	Na	67.8	23.3	1.0	7.6	1.02	2.569	23.47	892	41.5 ± 0.2
Si–Ca–Fe–K	K	68.3	22.9	1.0	7.8	1.38	2.565	24.49	962	37.1 ± 0.8
Si–Ca–Fe–Rb	Rb	67.9	22.8	1.0	8.0	1.52	2.768	25.41	989	35.3 ± 0.4
Si–Ca–Fe–Cs	Cs	67.7	23.2	1.0	7.9	1.67	3.011	25.81	1013	34.5 ± 0.8
Si–Ca–Fe	···	62.6	36.2	1.1	···	···	2.672	22.38	1007	n.d.[c]
Si–Na–Fe	Na	91.8	···	1.0	7.0	1.02	2.263	27.08	890	n.d.

[a] r_A is stated for a coordination number of 6 (Ref. 8). T_g and m have been determined by DSC and viscosity measurements, respectively.
[b] All iron is reported as Fe_2O_3.
[c] n.d.: not determined.

- Why are the alkali ions slower than the alkaline earth ions under these reducing conditions?
- Which alkali ion most effectively creates the silica-rich surface layer?

To answer these questions, we perform three types of diffusion experiments. First, glasses in the $SiO_2-CaO-Fe_2O_3-A_2O$ (A=Na, K, Rb, or Cs) series are heat-treated in the reducing H_2/N_2 (1/99 v/v) atmosphere for a given duration at various temperatures to determine the activation energy of Ca^{2+} diffusion as a function of the type of the alkali ion. Second, heat-treatments are performed at shorter durations compared to the previous experiments[2,7] in order to study the initial phases of the diffusion process. Third, glasses with and without alkali and alkaline earth ions, respectively, are compared in terms of their diffusion profiles. Furthermore, we investigate the effect of the alkali ions on the reduction reactions, density, glass transition temperature, and fragility of the iron-bearing silicate glasses. These results are used to gain insight into the observed diffusion phenomena. We also propose a simple model that accurately reproduces the relationship between glass transition temperature and fragility. Our model is based on the notion of temperature-dependent bond constraints, where the Vogel temperature serves as a rigidity percolation threshold. The success of this model confirms the universal topological origin of fragility.

II. EXPERIMENTAL

A. Sample preparation

Six glasses (see Table I) were prepared from analytical reagent-grade SiO_2, $CaCO_3$, Na_2CO_3, K_2CO_3, Rb_2CO_3, Cs_2CO_3, and Fe_2O_3 powders. The batches were mixed and melted at 1500 °C in an electric furnace (SF6/17, Entech) for 3 h in a $Pt_{90}Rh_{10}$ crucible. Afterwards, the glass melt was quenched on a brass plate and pressed to obtain cylindrical glasses of 7–10 cm diameter and ~5 mm height. The prepared glasses were annealed ~10 K above their respective glass transition temperatures for 10 min and then cooled naturally down to room temperature. We also attempted to prepare a lithium-containing glass in the $SiO_2-CaO-Fe_2O_3-A_2O$ series, but it was not possible due to phase separation. The Si–Ca–Fe–Na glass is the same as that used in another recent study.[7]

Cylindrical glass samples (diameter ~8–10 mm; thickness 3 mm) were prepared. The samples for the diffusion experiments were ground flat on one surface to a thickness of ~2 mm by a six-step procedure with SiC paper under ethanol. The surfaces were polished afterwards with 3 μm diamond paste and finally cleaned with acetone. To study the reduction reactions, ultraviolet-visible-near-infrared (UV-VIS-NIR) spectroscopy measurements were performed. The samples for these experiments were ground coplanar to achieve uniform thickness, and then they were polished to a thickness of 0.2 mm using the abovementioned procedure. Care was required during the sample preparation procedure as small bubbles and/or lack of uniformity of thickness affect the absorbance measurements.

B. Sample characterization

The chemical compositions of the glasses are listed in Table I. They were analyzed by x-ray fluorescence (XRF) on a S4-Pioneer spectrometer (Bruker-AXS). The main impurity in the glasses was Al_2O_3 (~0.2 mol %). Densities of the glasses were measured by He pycnometry (Porotech) and are also stated in Table I.

The glass transition temperature (T_g) was measured using a differential scanning calorimetry (DSC) instrument (STA 449C Jupiter, Netzsch). The isobaric heat capacity (C_p) curve for each measurement was calculated relative to the C_p curve of a sapphire reference material after subtraction of a correction run with empty crucibles. Measurements were carried out in a purged Ar atmosphere. The following heating procedure was carried out to determine T_g. First, the sample was heated at 10 K/min to a temperature ~1.11 times the respective T_g (in K) of each sample. Subsequently, the sample was cooled to room temperature at 10 K/min. Then, T_g was determined by a second upscan at 10 K/min in order to ensure a uniform thermal history of the glasses.[9] T_g was defined as the cross point between the extrapolated straight line of the glass C_p curve before the transition zone and the tangent at the inflection point of the sharp rise curve of C_p in the transition zone.

Viscosity was measured by beam-bending ($T > T_g$) and concentric cylinder ($T > T_{liquidus}$) experiments to determine the liquid fragility. For beam-bending experiments, bars of 45 mm length and 3×5 mm^2 cross-section were cut from the bulk glasses. The bars were bent in a symmetric three-point forced bending mode with 40 mm open span (VIS 401, Bähr). A 300 g weight was used to explore the viscosity range from approximately 10^{12}–$10^{9.5}$ Pa·s at a constant heating rate of 10 K/min. The viscosity was calculated according to DIN ISO 7884–4.[10] The low viscosities ($<10^3$ Pa·s) were measured using a concentric cylinder viscometer. The viscometer consisted of furnace, viscometer head, spindle, and sample crucible. The viscometer head (Physica Rheolab MC1, Paar Physica) was mounted on top of a high temperature furnace (HT 7, Scandiaovnen A/S). The spindle and crucible were made of $Pt_{80}Rh_{20}$. The viscometer was calibrated using the National Bureau of Standards 710A standard glass.

C. Thermal treatment

To induce the reduction reactions and diffusion processes, the polished glasses were heat-treated at 1 atm in an electric furnace under a flow of H_2/N_2 (1/99 v/v) gas. The glass samples were inserted into the cold furnace and the gas flow was turned on. The oxygen partial pressure was set to be a known value by using a Fe_3O_4/Fe_2O_3 redox buffer. Fe_2O_3 and Fe_3O_4 powders were mixed in the molar ratio 3:2 and placed into the furnace together with the samples. The furnace was then heated at 10 K/min to the predetermined heat-treatment temperature and kept at this temperature for a given duration. Afterwards, the furnace was cooled down to room temperature at 10 K/min.

The glasses in the SiO_2–CaO–Fe_2O_3–A_2O (A=Na, K, Rb, or Cs) series were treated at 0.95, 1.00, 1.025, and 1.05 times their respective T_g (in K) for 2 h, at their respective T_g for 60 h, and at the T_g (892 K) of the Si–Ca–Fe–Na glass for 60 h. Additionally, the Si–Ca–Fe–Na glass was treated at its T_g for 0.2, 1, 8, and 16 h, respectively. The ternary Si–Ca–Fe and Si–Na–Fe glasses were treated at their respective T_g for 2 h.

D. UV-VIS-NIR spectroscopy

Usually, iron in glasses exists in the states of Fe^{2+} and Fe^{3+}. In this work, UV-VIS-NIR absorption spectroscopy was used to determine the change in the valence state of iron of 0.20-mm-thick samples for the SiO_2–CaO–Fe_2O_3–A_2O (A=Na, K, Rb, or Cs) series. UV-VIS-NIR spectra were recorded over the wavelength range of 300–1100 nm using a UV-VIS-NIR Specord 200 spectrophotometer (Analytik Jena AG) at a resolution of 1 nm. The spectra were recorded with air as reference.

The ferrous (Fe^{2+}) ion has a broad absorption peak with maximum absorbance at 1050–1100 nm.[11,12] The position and maximum absorbance of this peak varies with glass composition and the absorption coefficients for our glasses were not known. Therefore, the absorption coefficient of the Lambert–Beer equation for the Si–Ca–Fe–Na glass was calculated: $A = c \cdot \varepsilon \cdot x$, where A is the absorbance, c is the concentration, ε is the absorption coefficient, and x is the sample thickness. In our previous study, the redox state $[Fe^{3+}]/[Fe_{tot}]$, where $[Fe_{tot}]=[Fe^{2+}]+[Fe^{3+}]$, of this glass was found by Mössbauer spectroscopy to be 77 ± 2 at. %.[7] By using the $[Fe^{3+}]/[Fe_{tot}]$ ratio and the total iron content, the concentration of ferrous iron was calculated in the untreated Si–Ca–Fe–Na glass. Plotting the absorbance near 1075 nm versus the sample thickness (0.12, 0.20, 0.40, and 0.80 mm) gave a linear relation ($R^2=0.995$). From the slope of this plot ($c \cdot \varepsilon$), the absorption coefficient was calculated to be 3.82 L mol^{-1} mm^{-1}.

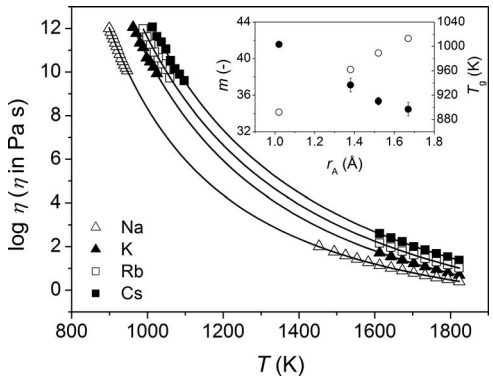

FIG. 1. Viscosity as a function of temperature for the SiO_2–CaO–Fe_2O_3–A_2O glasses with A=Na, K, Rb, or Cs. The data are fit with Eq. (1) and the values of the fragility index m are listed in Table I. The low and high temperature viscosity data have been measured by beam-bending and concentric cylinder viscometry, respectively. Inset: The fragility index m (closed circles) and the glass transition temperature T_g (open circles) determined by DSC as a function of the ionic radius r_A of the alkali ions.

E. Secondary neutral mass spectroscopy (SNMS)

To investigate the diffusion processes, compositional analysis of the surfaces was carried out using electron-gas SNMS. The measurements were performed on an INA3 (Leybold AG) instrument equipped with a Balzers QMH511 quadrupole mass spectrometer and a Photonics SEM XP1600/14 amplifier. The analyzed area had a diameter of 5 mm and was sputtered using Kr plasma with an energy of ~500 eV. The time dependence of the sputter profiles was converted into depth dependence by measuring the depth of the sputtered crater at 12 different directions on the same sample with a Tencor P1 profilometer.

III. RESULTS

Figure 1 shows the dependence of viscosity η on temperature T for the SiO_2–CaO–Fe_2O_3–A_2O glasses with A=Na, K, Rb, or Cs. An increase in viscosity with increasing ionic radius r_A of the alkali ion at a given temperature is observed for both the low and high temperature data. To determine the liquid fragility index, we fit the viscosity data with the Mauro–Yue–Ellison–Gupta–Allan (MYEGA) equation,[13]

$$\log \eta = \log \eta_\infty + (12 - \log \eta_\infty)\frac{T_g}{T} \times \exp\left[\left(\frac{m}{12 - \log \eta_\infty} - 1\right)\left(\frac{T_g}{T} - 1\right)\right], \quad (1)$$

where η_∞ is the extrapolated viscosity at infinite temperature and m is the fragility of the glass-forming liquid. Fragility is defined as the slope of the log η versus T_g/T curve at T_g,[14,15]

$$m \equiv \left.\frac{d \log \eta}{d(T_g/T)}\right|_{T=T_g}. \quad (2)$$

In the model, the viscosity at the glass transition temperature T_g is set equal to 10^{12} Pa·s since this has been shown to be equivalent to the calorimetrically measured T_g values for oxide glasses.[16] We have previously shown that the MYEGA equation offers improved accuracy in performing low temperature extrapolations compared to the Vogel–Fulcher–Tammann (VFT)[17–19] and Avramov–Milchev (AM)[20,21] equations.[13] VFT and AM lead to systematic overprediction or underprediction of fragility, respectively, whereas the MYEGA equation exhibits no such systematic error.[13] Here, we have also tested the abovementioned three equations on the four glasses in the SiO_2–CaO–Fe_2O_3–A_2O series regarding their ability to fit the viscosity data using a Levenberg–Marquardt algorithm. The results again show that MYEGA describes the viscosity data better than the other two equations. In detail, the average standard deviation for the four glasses are 0.036, 0.043, and 0.041 in log(Pa·s) for MYEGA, VFT, and AM, respectively. Hence, we apply the MYEGA equation of Eq. (1) to fit the viscosity data of the four glasses as shown in Fig. 1. The fitted values of m are listed in Table I and shown in the inset of Fig. 1 as a function of r_A. For the glass melts in the series SiO_2–CaO–Fe_2O_3–A_2O with A=Na, K, Rb, or Cs, the fragility decreases with increasing size of the alkali ion. In contrast, the glass transition temperature increases with r_A (see Table I and inset of Fig. 1).

UV-VIS-NIR spectra of untreated and heat-treated glasses in the SiO_2–CaO–Fe_2O_3–A_2O (A=Na, K, Rb, or Cs) series are shown in Figs. 2(a) and 2(b). A maximum absorption peak is found at approximately 1075 nm, which is due to the presence of Fe^{2+} ions.[11,12] Only the untreated glass with A=Na is shown in the figure, but the maximum absorbance and position of the Fe^{2+} peak is the same (within ±5%) for all untreated glasses. This indicates that the initial $[Fe^{3+}]/[Fe_{tot}]$ ratio is approximately the same in all the glasses. This has been additionally confirmed by performing thermogravimetric measurements on the glasses. The mass increase due to incorporation of oxygen was the same (within ±6%) for all six glasses. By using ^{57}Fe Mössbauer spectroscopy, we have previously shown that the untreated Si–Ca–Fe–Na glass contains 77±2% of its Fe ions as Fe^{3+}.[7]

To study the kinetics of the reduction reaction, the Si–Ca–Fe–Na glass has been heat-treated at its T_g of 892 K for 2, 8, 16, and 60 h [Fig. 2(a)]. With increasing treatment duration t_a, the absorbance of the Fe^{2+} band increases because Fe^{3+} is reduced to Fe^{2+}. The change in Fe^{2+} concentration increases approximately linearly with the square root of the treatment duration, implying that diffusion-controlled kinetics occurs [see inset of Fig. 2(a)]. Figure 2(b) shows UV-VIS-NIR spectra of the SiO_2–CaO–Fe_2O_3–A_2O (A=Na, K, Rb, or Cs) glasses heat-treated at their respective T_g for 60 h and at the T_g of the Si–Ca–Fe–Na glass (892 K) for 60 h. When the glasses are treated at the same temperature, the change in absorbance of the Fe^{2+} peak increases with increasing radius of the alkali ion. When the glasses are treated at their respective T_g, the trend is qualitatively the same but the differences between the glasses are more pronounced. This is because the Si–Ca–Fe–Cs glass has the highest T_g and therefore it is treated at the highest temperature.

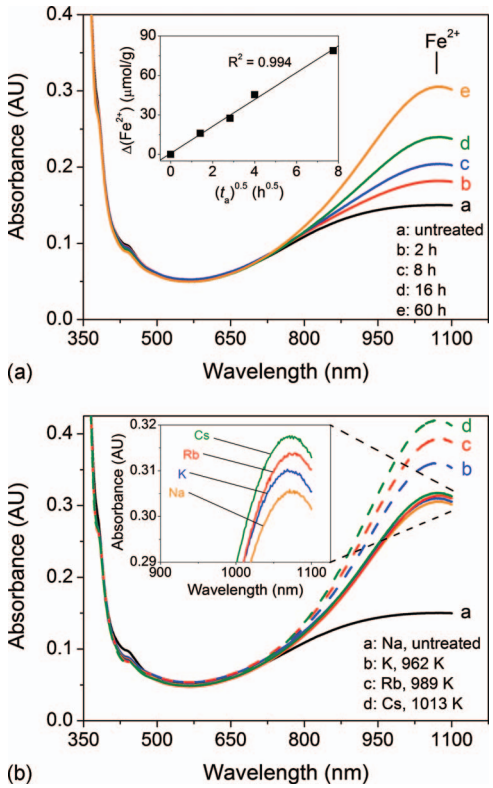

FIG. 2. UV–VIS–NIR spectra of 0.20-mm-thick glass samples. The band positioned near 1075 nm is due to a $d \rightarrow d$ transition of Fe^{2+}. (a) Untreated and heat-treated SiO_2–CaO–Na_2O–Fe_2O_3 glasses. The treatments have been performed in H_2/N_2 (1/99) at T_g=892K for various durations. The inset shows the change in Fe^{2+} concentration $[\Delta(Fe^{2+})]$ as a function of the square root of the treatment duration $(t_a^{0.5})$. For the glass treated for 8 h, $\Delta(Fe^{2+})$ was determined by three independent measurements. Based on these results, the accuracy of the determination of $\Delta(Fe^{2+})$ is estimated to be ±4 μmol/g. (b) Untreated and heat-treated SiO_2–CaO–Fe_2O_3–A_2O glasses with A=Na, K, Rb, or Cs. The glasses have all been treated in H_2/N_2 (1/99) at their respective T_g for 60 h and at 892 K for 60 h. The inset enlarges the region with the glasses treated at 892 K for 60 h.

The SNMS technique has been employed to study the reduction-induced diffusion processes in the six glasses. The method provides information about the surface composition of the glass as a function of depth. Selected depth profiles are shown in Figs. 3(a)–3(d). Figure 3(a) shows the depth profile of the Si–Ca–Fe–K glass that has been heat-treated in H_2/N_2 (1/99) for 2 h at $1.05T_g$=1010 K. A depletion of calcium, potassium, and iron is observed near the surface. The extent of the calcium depletion is larger than that of potassium and iron. Qualitatively all six glasses display the same type of surface depletion of network-modifying cations as a result of

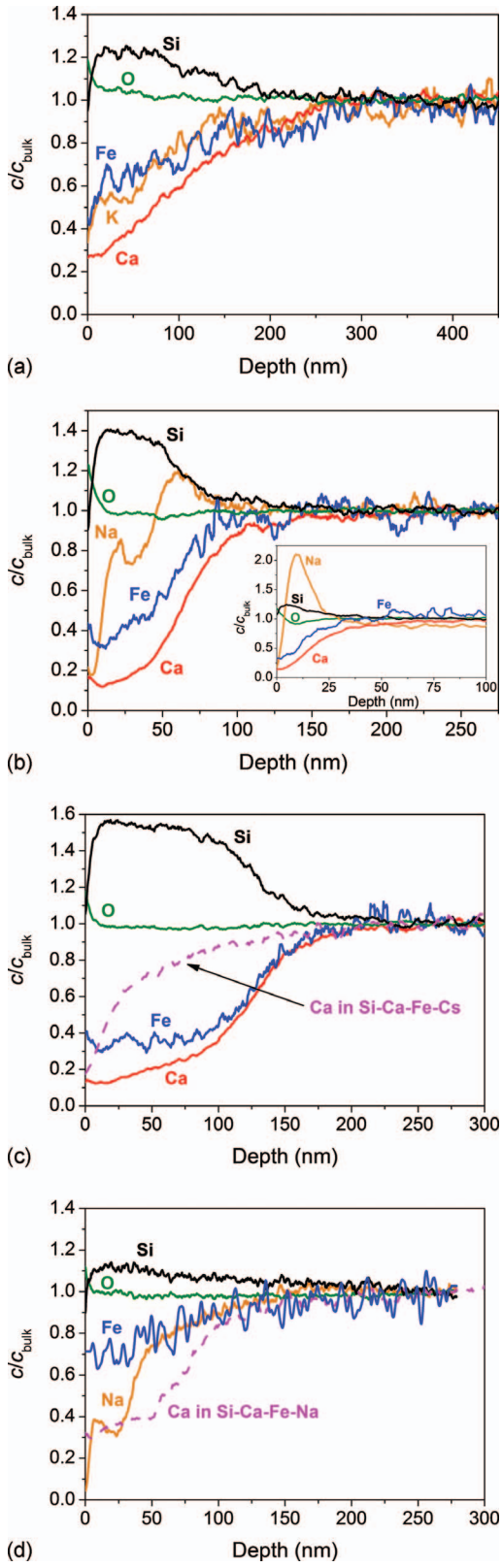

FIG. 3. SNMS depth profiles of the various glasses in Table I heat-treated in H_2/N_2 (1/99). The curves are plotted as concentration of the element at a given depth divided by the concentration of the same element in the bulk of the glass (c/c_{bulk}). (a) Si–Ca–Fe–K glass treated for 2 h at $1.05T_g$ =1010 K. (b) Si–Ca–Fe–Na glass treated for 1 h at T_g=892 K. Inset: The same glass treated at 892 K for 0.2 h. (c) Si–Ca–Fe glass treated for 2 h at T_g=1007 K. The dashed curve shows the Ca profile in the Si–Ca–Fe–Cs glass treated for 2 h at its T_g=1013 K. (d) Si–Na–Fe glass treated for 2 h at T_g=890 K. The dashed curve shows the Ca profile in the Si–Ca–Fe–Na glass treated for 2 h at its T_g=892 K.

heat-treatment for 2 h at temperatures around their respective T_g. The surface depletion is caused by an inward diffusion of these ions induced by the reduction of Fe^{3+} to Fe^{2+}.[2,3] An important consequence of the inward diffusion is the creation of a silica-rich surface layer as seen in Figs. 3(a)–3(d).[2,22] Before heat-treatment in H_2/N_2 (1/99), the glasses do not show any variation in composition as a function of depth.

To study the initial phases of the diffusion process, the Si–Ca–Fe–Na glass has been heat-treated at its T_g for 1 h [Fig. 3(b)] and 0.2 h [inset of Fig. 3(b)]. The glass treated for 0.2 h displays a ~50 nm layer depleted in calcium and iron, whereas the concentrations of silicon and sodium are higher in this layer than in the bulk. When the duration of the treatment is increased to 1 h, the thickness of the layer depleted in calcium and iron increases and inward diffusion of sodium occurs. Furthermore, an enrichment of sodium is observed in the depth interval from approximately 50–100 nm. The ternary Si–Ca–Fe [Fig. 3(c)] and Si–Na–Fe [Fig. 3(d)] glasses have been heat-treated at their respective T_g for 2 h. Inward diffusion of Ca^{2+} and Na^+, respectively, is also observed in these glasses.

For the SiO_2–CaO–Fe_2O_3–A_2O (A=Na, K, Rb, or Cs) glass series, the temperature dependence of the calcium diffusion has been systematically investigated. To quantitatively analyze the effect of the alkali ion on the diffusion of Ca^{2+}, the diffusion depth ($\Delta\xi$) of Ca^{2+} is calculated as the first depth at which $c/c_{bulk} \geq 1$ for three measurements in succession. To estimate the uncertainty of the diffusion depths values, three independent SNMS measurements on the Si–Ca–Fe–Na glass heat-treated in H_2/N_2 (1/99) for 2 h at $1.05T_g$ =937 K have been performed. Based on the SNMS depth profiles, the uncertainty range of $\Delta\xi$ is found to be approximately ±10 nm. Since we have previously shown that the inward cationic diffusion of alkaline earth ions is parabolic with time,[2,7] we calculate the rate constant k' of the calcium diffusion[23]

$$k' = \frac{(\Delta\xi)^2}{t_d}, \tag{3}$$

where t_d is the diffusion time (2 h). k' is proportional to the product of the diffusion coefficient of the rate-limiting species (divalent cation) and a thermodynamic driving force (gradient in oxygen activity).[4] The divalent cations are the rate-limiting species for the reduction process since they diffuse faster than the monovalent cations. The inward diffusion of the cations charge-balances the outward flux of electron holes and the mobility of electron holes is much larger than that of cations. Hence, from the temperature sensitivity of k' and gradient in oxygen activity,[2] the activation energy of calcium diffusion (E_d) can be obtained by plotting the data in Arrhenius coordinates as shown in Fig. 4. The diffusion data for each glass reveal an Arrhenius dependence on temperature in the studied temperature range, which is indicated by the solid lines in Fig. 4 ($R^2 > 0.98$). E_d is calculated from the slope of each line and is plotted as a function of the ionic radius of the alkali ion in the inset of Fig. 4. The error bars of E_d correspond to the standard deviation in determining E_d from the linear fit. E_d decreases with increasing size of the alkali ion.

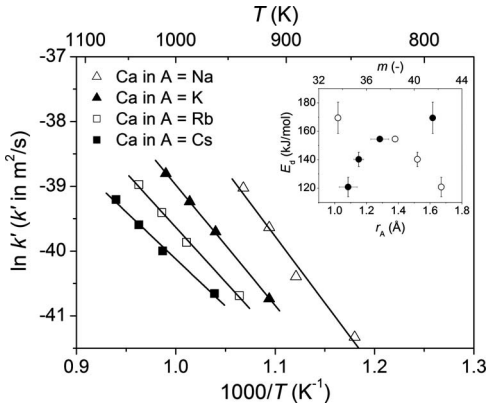

FIG. 4. Arrhenius plot of $\ln k'$ as a function of the reciprocal absolute temperature of the $SiO_2-CaO-Fe_2O_3-A_2O$ (A=Na, K, Rb, or Cs) glasses that have been heat-treated in H_2/N_2 (1/99) at different temperatures for 2 h. Inset: The activation energy of calcium diffusion E_d as a function of both the ionic radius r_A of the alkali ions (open circles) and the fragility index m (closed circles).

IV. DISCUSSION

A. Effect of alkali ion on density, T_g, and fragility

Density, glass transition temperature, and fragility vary as a function of the type of the alkali ion in the $SiO_2-CaO-Fe_2O_3-A_2O$ (A=Na, K, Rb, or Cs) series (Table I). The changes cannot be ascribed to differences in the content of nonbridging oxygen ions since these differences are negligible due to negligible composition fluctuations caused during sample preparation and XRF measurements. The changes cannot be attributed to differences in the hydroxyl content either since it is predominantly affected by the melting conditions,[24] which are the same for all the four glasses. The initial Fe^{3+} content affects the inward cationic diffusion process,[2,3] but the content has been found to be approximately the same for the four glasses. Therefore, the observed glass property changes can be ascribed to the difference in size of the alkali ions, and hence, to their impact on the glass network structure.

For the glasses containing K, Rb, and Cs, the density increases with increasing atomic weight of the alkali ion. However, the density of the Si–Ca–Fe–Na glass is approximately the same as that of the Si–Ca–Fe–K glass even though a potassium ion weighs almost doubly as much as a sodium ion. This trend has previously been reported[25] and it can be ascribed to an increase in molar volume of the structure imposed by the large, lower field strength ions. In Table I, the molar volumes are calculated based on the density and composition data. The glass transition temperature T_g of the glasses increases with increasing size of the alkali ion r_A even though the polymerization degree is the same for all the glasses (see inset of Fig. 1). For alkaline earth ions, it has previously been reported that T_g decreases when the size of the alkaline earth ion increases.[7,26] This is explained by a weakening of the overall network because an increase in alkaline earth radius leads to a decrease in the field strength of these ions. Hence, the attraction of alkaline earth ions to their surrounding structural groups of $[SiO_4]$ tetrahedra is reduced. The alkali ions are not as strongly associated with the glass network as the alkaline earth ions. Therefore, it is inferred that the increase in T_g with increasing r_A might be attributed to a weakening of the A–O bonds and a corresponding strengthening of the Si–O bond constraints in the glass network.

Similar arguments as those used above can explain why the studied glass melts become less fragile with increasing r_A. The high degree of short range order created by the large alkali ions prevents a rapid breakdown of the bond constraints with increasing temperature, e.g., the Cs-containing liquid is relatively strong. In other words, the skeleton-network regions become more dominant compared to the floppy regions. To quantitatively account for the correlation between fragility and glass transition temperature, we begin with the MYEGA model of Eq. (1), which may be written in a simplified form as[13]

$$\log\ \eta = \log\ \eta_\infty + \frac{K}{T}\exp\left(\frac{C}{T}\right), \tag{4}$$

where K and C are constants for a given composition. As discussed in detail by Mauro *et al.*,[13] K is a normalized activation barrier for structural rearrangements and C is the temperature at which a topological floppy-to-rigid transition occurs upon cooling. In the high temperature limit, the exponential of Eq. (4) can be expanded as a Taylor series,

$$\log\ \eta = \log\ \eta_\infty + \frac{K}{T\exp(-C/T)} \approx \log\ \eta_\infty + \frac{K}{T(1-C/T)}. \tag{5}$$

This is exactly the empirical VFT form of viscosity.[17–19] Hence, VFT can be derived as a simple approximation to MYEGA.

While the MYEGA equation is more quantitatively accurate, especially at low temperatures, the approximate VFT form is useful for deriving a simple analytical relation between fragility and glass transition temperature. Defining the Vogel temperature $T_0=C$ and $D_0=K/T_0$, we have

$$\log\ \eta = \log\ \eta_\infty + \frac{1}{T}\frac{D_0T_0}{(1-T_0/T)}. \tag{6}$$

VFT predicts a divergence of viscosity at the Vogel temperature T_0. Following the Adam–Gibbs model, such divergence corresponds to a vanishing of the configurational entropy at T_0. Hence, T_0 has often been found to be coincident with the Kauzmann temperature T_K,[27–29] which is the temperature at which the extrapolated liquid entropy apparently intersects that of the crystal.[30] The entropy catastrophe at T_K and the corresponding dynamic divergence at T_0 are controversial issues. According to the energy landscape view, a liquid cannot be confined in a single microstate at a finite temperature, and so the entropy cannot truly vanish unless the system is cooled completely to absolute zero.[31] Therefore, based on the recent work of Gupta and Mauro,[32] it seems more appropriate to associate T_0 with a rigidity percolation threshold temperature at which the system becomes optimally constrained. In other words, T_0 is the temperature at which the number of frozen-in constraints exactly equals the number of degrees of freedom. At higher temperatures, the number of network constraints is low and the network is "floppy," but as the

temperature is lowered, more constraints become frozen in[33–36] until all the floppy modes vanish at T_0. Since most of the configurational entropy is associated with floppy modes,[37] the configurational entropy also "mostly" vanishes at T_0. This notion of T_0 as a rigidity percolation temperature also directly follows from our derivation of VFT from MYEGA in Eq. (5), since the MYEGA parameter C is the temperature at which the floppy-to-rigid transition occurs.[13]

The recent work of Carmi *et al.*[38] has also proposed T_K as percolation transition temperature (T_p). By studying the energy landscape of the glass network at different temperatures, the authors argue that at T_p, the system is bound to a region in phase space that corresponds to the ideal glass state, i.e., the space of configurations is broken down into disconnected components (network disintegrates). At high temperatures, the network is intact as the system has sufficient thermal energy to access most states. At lower temperatures, the network becomes increasingly disintegrated until the percolation threshold is reached when the energy barriers become almost impossible to cross.[38] Making the connection $T_0=T_K=T_p$, the Vogel temperature T_0 could also be associated with this percolation transition.

For the studied $SiO_2–CaO–Fe_2O_3–A_2O$ (A=Na, K, Rb, or Cs) glass series, the molar ratios between different components are the same, but the type of alkali ion is different. In our previous work,[7] we studied the glass series $SiO_2–RO–Fe_2O_3–Na_2O$ (R=Mg, Ca, Sr, or Ba) with the same composition as that of the alkali series, i.e., the same glass corresponds to A=Na and R=Ca. If the ions play the same topological role in the glass network, the glasses should become isostatic and percolation break down at approximately the same temperature upon cooling, i.e., T_0 should be a constant. Based on the measured values of T_g and m, we can test if this is the case by obtaining an equation containing only T_0, T_g, and m. First, we set the viscosity at T_g and infinite temperature equal to 10^{12} and $10^{-3.5}$ Pa·s, respectively.[16] Then, from Eq. (6) we have

$$D_0 = \frac{15.5(T_g - T_0)}{T_0}. \tag{7}$$

This expression for D_0 is now substituted back into Eq. (6). The slope of the log η versus T_g/T curve is then

$$\frac{d \log \eta}{d(T_g/T)} = \frac{15.5(T_g - T_0)}{T_g(1 - T_0/T)}\left(1 + \frac{T_0}{T - T_0}\right). \tag{8}$$

The fragility m is defined by Eq. (2). We may thus write m as a function of T_g and T_0 by introducing Eq. (8) into Eq. (2), which yields

$$m = 15.5\left(1 + \frac{T_0}{T_g - T_0}\right). \tag{9}$$

We now use the glass with A=Na (i.e., R=Ca) as a reference. Using the values of T_g and m from Table I and solving Eq. (9) for T_0 gives T_0=559 K. Inserting this value into Eq. (9) gives the solid line in Fig. 5, in which m is plotted as a function of T_g. Except for the magnesium-containing glass, the agreement of the data with the model is nearly perfect. It should be noticed that the model contains no fitting parameters, i.e., only the Si–Ca–Fe–Na glass has been picked as a reference. The nearly perfect fit is a good verification of the temperature-dependent network constraint model of Mauro and co-workers[32,39] and the universal role of network topology in governing liquid fragility. The fact that the Mg data point falls off the curve may be explained by the special role that Mg plays in the glass network compared to the larger alkaline earth ions. The presence of fourfold and fivefold coordinated Mg^{2+} in various silicate glass compositions has been reported,[40–42] whereas the larger alkaline earth ions are expected only to occur in sixfold coordination. Hence, the results presented in Fig. 5 provides additional evidence of the unique topological role that Mg plays in a glass. This is also coincident with the fact that the diffusion of Mg^{2+} is fastest in the redox-induced diffusion processes.[7,43]

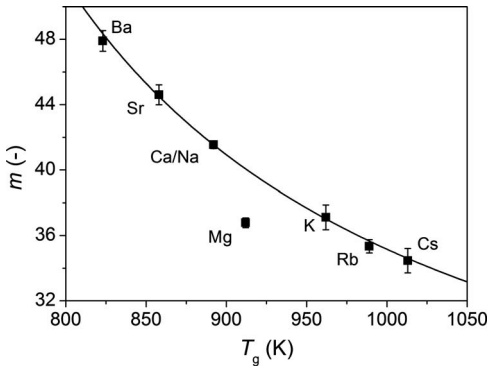

FIG. 5. The fragility index m plotted as a function of the glass transition temperature T_g for the glasses $SiO_2–CaO–Fe_2O_3–A_2O$ with A=Na, K, Rb, or Cs, and $SiO_2–RO–Fe_2O_3–Na_2O$ with R=Mg, Ca, Sr, or Ba (Ref. 7). Notice that the same glass corresponds to A=Na and R=Ca. T_g has been determined by DSC. m has been determined by fitting the measured viscosity data to Eq. (1). The solid line corresponds to Eq. (9) using the glass with A=Na (R=Ca) as a reference.

B. Effect of alkali ion on redox-diffusion processes

When the glasses in the $SiO_2–CaO–Fe_2O_3–A_2O$ (A=Na, K, Rb, or Cs) series are heat-treated at the T_g of the Si–Ca–Fe–Na glass (i.e., at the same temperature), the order of the degree of reduction [inset of Fig. 2(b)] follows the same trend as that of the molar volume of these glasses (Table I). Since the modifier ions are believed to occupy interstitial sites in the network, they block the paths for the small H_2 molecules. Hence, when the glass structure is relatively open, it is easier for the H_2 molecules to permeate the glass. In comparison, the diffusion data in Fig. 4 show that the isothermal inward diffusion of Ca^{2+} is fastest in the Si–Ca–Fe–Na glass, i.e., in the glass with the lowest molar volume. This is because two simultaneous processes contribute to the reduction of Fe^{3+} to Fe^{2+}: H_2 permeation and outward flux of electron holes. The former process dominates the reduction reaction at 0.01 bar of H_2.[2] Therefore, the thickness of the modified surface layer (as measured by SNMS) cannot be directly correlated with the degree of reduction (as measured by UV-VIS-NIR spectroscopy). In other words, a large extent of Fe^{3+} reduction does not necessarily result in a thick silica-rich surface layer because two processes contribute to the reduction in Fe^{3+}.

There must therefore be another reason for why large alkali ions cause the slowest isothermal Ca^{2+} diffusion in the glasses. The Si–Ca–Fe–Cs glass has the highest T_g of the glasses and it has previously been shown that this type of redox-induced diffusion begins at temperatures around $0.8T_g$ (in K).[44] Apparently, the process requires some degree of viscous softening even though the motion of the alkaline earth ions is decoupled from that of the network.[7] Therefore, the glass with highest T_g will have the slowest Ca^{2+} diffusion when the glasses are heat-treated at the same temperature.

The temperature sensitivity of the Ca^{2+} diffusion shows that the diffusion activation energy (E_d) decreases with increasing r_A (inset of Fig. 4). In our previous work,[7] we predicted the presence of interconnected channels in the glass network based on the modified random network model of Greaves.[45] We found that the alkaline earth diffusion can be enhanced by lowering the liquid fragility due to the more simple diffusion paths in strong systems. This could also explain the results in this study since there is a positive correlation between E_d and m in the SiO_2–CaO–Fe_2O_3–A_2O (A=Na, K, Rb, or Cs) series (inset of Fig. 4).

Regarding the inward diffusion, the results obtained in this study clearly demonstrate that alkali ions diffuse slower than the divalent calcium ions. In the beginning of the process, the alkali ions have not started to diffuse to any significant extent and the diffusion of Ca^{2+} and Fe^{2+} completely dominates, which is shown in Fig. 3(b). The high concentration of sodium in the surface layer of these glasses is caused by the inward diffusion of calcium and iron. Independent diffusion processes of monovalent and divalent cations therefore occur in the beginning stage, whereas parallel diffusion processes of various cations occurs at a later stage. Figure 3(d) shows that the Ca^{2+} diffusion is faster than that of Na^+ since the extent of Ca^{2+} diffusion in the Si–Ca–Fe–Na glass is larger than that of Na^+ in the ternary Si–Na–Fe glass. The two glasses are comparable since they have approximately the same T_g. Furthermore, Fig. 3(c) illustrates that the presence of alkali ions decreases the diffusivity of the alkaline earth ions because the extent of Ca^{2+} diffusion is smaller in the Si–Ca–Fe–Cs glass than in the ternary Si–Ca–Fe glass. These two glasses also have approximately the same T_g. It should be noticed that the diffusion extent could also depend on the Ca^{2+}/Fe^{3+} ratio because Ca^{2+} diffuses to charge-balance the outward flux of electron holes. The ratio is higher for the Si–Ca–Fe glass than for the Si–Ca–Fe–Cs glass, but this difference in Ca^{2+}/Fe^{3+} ratio should result in a higher diffusivity of Ca^{2+} in the Si–Ca–Fe–Cs glass.[2,3] Thus, the presence of relatively slow alkali ions may block the diffusion of the faster alkaline earth ions in the interconnected channels, i.e., the slow alkali ions occupy interstices and hereby increase the packing density. These interstices can no longer be used for alkaline earth migration.

The reason why the alkaline earth ions diffuse faster than the alkali ions could be the following. In general, ionic diffusion in solids proceeds via jumps between different structural sites. The localized energy landscape experienced by the ion in a glass has a distribution of energy barriers with various heights. The ion spends most of its time vibrating about a potential energy minimum, and an interbasin transition occurs when sufficient energy is available to overcome the barrier. In the reduction-induced cationic diffusion process, the gradient in oxygen activity is the driving force for the cationic diffusion. The gradient is dissipated by electron hole movement from Fe^{3+} to Fe^{2+}. The electron hole creates a structural distortion (polaron).[46] The distorted domain moves with the electron hole between localized electronic states, whereas the cation moves in the opposite direction. The polaron motion is much faster than that of both alkali and alkaline earth ions in glasses.[46] Therefore, the rate of the inward diffusion depends on the degree of the ease of the joint motion of the ions with the polaron. The alkaline earth ions should diffuse faster than alkali ion because the former ones are able to carry more positive charges than the latter ones to charge-balance the flux of electron holes. An alkaline earth ion neutralizes two electron holes, whereas an alkali ion neutralizes only one electron hole. This argument would then lead to the assumption that trivalent modifier ions (e.g., Al^{3+}) are more mobile than the alkaline earth ions. But this is not the case[43] because the former ones are more strongly bound to the oxygen anions. For the case of the alkaline earth ions, the charge-balancing capability turns out to be a predominant effect in comparison to the effect of cation-oxygen bond strength that hinders the divalent ionic diffusion. It should be mentioned that the diffusion coefficient of the alkali ions is smaller in the inward diffusion process compared to what is found in the literature because the latter results have predominantly been obtained by the use of a radioactive tracer.[25] For the alkaline earth ions, good agreement between the inward diffusion data and tracer diffusion data have been reported.[2–4]

V. CONCLUSIONS

We have studied the impact of alkali ions on the diffusion of calcium ions in the glass transition range in iron-bearing silicate glasses. The diffusion is induced by thermally treating the glasses in a reducing atmosphere at temperatures around T_g. This treatment causes a reduction of Fe^{3+} to Fe^{2+}, which requires an inward diffusion of mobile cations. We have found that the mobility of Ca^{2+} strongly depends on the type of the alkali ion present in the glass and that the diffusion of Ca^{2+} is faster than that of the alkali ions. The presence of alkali ions decreases the mobility of Ca^{2+} and the activation energy of Ca^{2+} diffusion decreases with increasing radius of the alkali ion. The latter trend is coincident with a decrease in liquid fragility and an increase in glass transition temperature. Furthermore, based on the concepts of the temperature-dependent network constraint model, we have proposed a simple model to explain the correlation between fragility and glass transition temperature of the alkali-alkaline earth silicate glasses. The glass containing magnesium deviates from the general trend, confirming the special topological role of Mg^{2+} in oxide glasses.

ACKNOWLEDGMENTS

The authors acknowledge Thomas Peter and Michael Zellmann (Clausthal University of Technology) for performing SNMS and XRF measurements, respectively. They ac-

knowledge Martin Jensen (Aalborg University) for assistance with glass preparation and Joachim Deubener (Clausthal University of Technology) for supporting experiments. This work was supported by the International Doctoral School of Technology and Science at Aalborg University under Ph.D. Stipend No. 562/06-FS-28045.

[1] A. K. Varshneya, *Fundamentals of Inorganic Glasses* (Society of Glass Technology, Sheffield, 2006).
[2] M. M. Smedskjaer and Y. Z. Yue, J. Non-Cryst. Solids **355**, 908 (2009).
[3] M. M. Smedskjaer and Y. Z. Yue, Solid State Ionics **180**, 1121 (2009).
[4] R. L. A. Everman and R. F. Cooper, J. Am. Ceram. Soc. **86**, 487 (2003).
[5] F. Natrup, H. Bracht, S. Murugavel, and B. Roling, Phys. Chem. Chem. Phys. **7**, 2279 (2005).
[6] E. M. Tanguep Nijokep and H. Mehrer, Solid State Ionics **177**, 2839 (2006).
[7] M. M. Smedskjaer, Y. Z. Yue, J. Deubener, and H. P. Gunnlaugsson, J. Phys. Chem. B **113**, 11194 (2009).
[8] R. D. Shannon, Acta Crystallogr., Sect. A: Cryst. Phys., Diffr., Theor. Gen. Crystallogr. **32**, 751 (1976).
[9] Y. Z. Yue, J. Non-Cryst. Solids **354**, 1112 (2008).
[10] DIN ISO 7884–4, *Viskosität und viskosimetrische Festpunkte. Teil 4: Bestimmung der Viskosität durch Balkenbiegen* (in German) (1987).
[11] A. Montenero, M. Friggeri, D. C. Giori, N. Belkhiria, and L. D. Pye, J. Non-Cryst. Solids **84**, 45 (1986).
[12] C. Ades, T. Toganidis, and J. P. Traverse, J. Non-Cryst. Solids **125**, 272 (1990).
[13] J. C. Mauro, Y. Z. Yue, A. J. Ellison, P. K. Gupta, and D. C. Allan, Proc. Natl. Acad. Sci. U.S.A. **106**, 19780 (2009).
[14] C. A. Angell, J. Non-Cryst. Solids **131–133**, 13 (1991).
[15] C. A. Angell, Science **267**, 1924 (1995).
[16] Y. Z. Yue, J. Non-Cryst. Solids **355**, 737 (2009).
[17] H. Vogel, Z. Phys. **22**, 645 (1921).
[18] G. S. Fulcher, J. Am. Ceram. Soc. **8**, 339 (1925).
[19] G. Tammann and W. Hesse, Z. Anorg. Allg. Chem. **156**, 245 (1926).
[20] I. Avramov, J. Non-Cryst. Solids **238**, 6 (1998).
[21] I. Avramov, J. Non-Cryst. Solids **351**, 3163 (2005).
[22] M. M. Smedskjaer, J. Deubener, and Y. Z. Yue, Chem. Mater. **21**, 1242 (2009).
[23] H. Schmalzried, *Solid State Reactions* (Verlag Chemie, Weinheim, 1984).
[24] F. Geotti-Bianchini and L. De Riu, Glastech. Ber. **71**, 230 (1998).
[25] J. E. Shelby, *Introduction to Glass Science and Technology* (The Royal Society of Chemistry, Cambridge, 2005).
[26] F. V. Natrup and H. Bracht, Phys. Chem. Glasses **46**, 95 (2005).
[27] C. A. Angell and D. L. Smith, J. Phys. Chem. **86**, 3845 (1982).
[28] P. Dixon, Phys. Rev. B **42**, 8179 (1990).
[29] C. A. Angell, L. Boehm, M. Oguni, and D. L. Smith, J. Mol. Liq. **56**, 275 (1993).
[30] W. Kauzmann, Chem. Rev. (Washington, D.C.) **43**, 219 (1948).
[31] F. H. Stillinger, J. Chem. Phys. **88**, 7818 (1988).
[32] P. K. Gupta and J. C. Mauro, J. Chem. Phys. **130**, 094503 (2009).
[33] J. C. Phillips, J. Non-Cryst. Solids **34**, 153 (1979).
[34] J. C. Phillips and M. F. Thorpe, Solid State Commun. **53**, 699 (1985).
[35] H. He and M. F. Thorpe, Phys. Rev. Lett. **54**, 2107 (1985).
[36] Y. Cai and M. F. Thorpe, Phys. Rev. B **40**, 10535 (1989).
[37] G. G. Naumis, J. Non-Cryst. Solids **352**, 4865 (2006).
[38] S. Carmi, S. Havlin, C. M. Song, K. Wang, and H. A. Makse, J. Phys. A: Math. Theor. **42**, 105101 (2009).
[39] J. C. Mauro, P. K. Gupta, and R. J. Loucks, J. Chem. Phys. **130**, 234503 (2009).
[40] S. Kroeker and J. F. Stebbins, Am. Mineral. **85**, 1459 (2000).
[41] M. C. Wilding, C. J. Benmore, J. A. Tangeman, and S. Sampath, Europhys. Lett. **67**, 212 (2004).
[42] N. Trcera, D. Cabaret, S. Rossano, F. Farges, A.-M. Flank, and P. Lagarde, Phys. Chem. Miner. **36**, 241 (2009).
[43] Y. Z. Yue, M. Korsgaard, L. F. Kirkegaard, and G. Heide, J. Am. Ceram. Soc. **92**, 62 (2009).
[44] L. F. Kirkegaard, M. Korsgaard, and Y. Z. Yue, Glass Sci. Technol. (Amsterdam, Neth.) **78**, 1 (2005).
[45] G. N. Greaves, J. Non-Cryst. Solids **71**, 203 (1985).
[46] G. B. Cook and R. F. Cooper, Am. Mineral. **85**, 397 (2000).